Polariton quantum blockade in a photonic dot

A. Verger,[1] C. Ciuti,[1,*] and I. Carusotto[2]
[1]*Laboratoire Pierre Aigrain, Ecole Normale Supérieure, 24, rue Lhomond, 75005 Paris, France*
[2]*CNR-INFM BEC Center and Dipartimento di Fisica, Università di Trento, I-38050 Povo, Italy*
(Received 15 February 2006; published 12 May 2006)

We investigate the quantum nonlinear dynamics of a resonantly excited photonic quantum dot embedding a quantum well in the strong exciton-photon coupling regime. Within a master equation approach, we study the polariton blockade effect due to polariton-polariton interactions as a function of the photonic dot geometry, spectral linewidths and energy detuning between quantum well exciton and confined photon mode. The second order coherence function $g^{(2)}(t,t')$ and the photon antibunching are calculated for both continuous wave and pulsed excitations.

DOI: 10.1103/PhysRevB.73.193306 PACS number(s): 42.50.−p, 42.65.−k, 71.36.+c, 03.65.−w

Several recent developments in the field of quantum information[1] and quantum communication[2] are based on light beams with strongly nonclassical properties. Many techniques have been investigated to obtain such beams, using, e.g., parametric down-conversion processes in bulk nonlinear crystals,[1] colored centers in diamond[3] or by taking advantage of semiconductor electronic quantum nanodots.[4–8]

Quantum wells strongly coupled to planar microcavities combine strong nonlinearities due to exciton-exciton interactions with an efficient coupling to radiation. In particular, their use as parametric amplifiers and oscillators working at low pump intensities appears promising.[9–14] Very recently, lithographic techniques have been developed to create high quality photonic dots able to confine the photon without spoiling the strong-coupling with the quantum well exciton. In this way, polaritons result confined in all three dimensions, with a vacuum Rabi splitting as large as several meVs.[15,16]

In this paper, we discuss the nonclassical properties of the light emitted by a resonantly excited polariton quantum dot. If the photonic confinement volume is small enough, the presence of just one polariton can block the resonant injection of a second polariton, since the polariton-polariton interaction shifts the resonance frequency by an amount of the order of the linewidth or even larger. The emitted light is, therefore, strongly anti-bunched. If a pulsed excitation beam is used, the present system can be used as a single-photon light emitter. In particular, the short radiative emission time (of the order of a few ps) makes it attractive for high-speed applications. The quantum polariton blockade effect here considered is reminiscent of the one proposed for atomic matter waves[17] and for photons in cavities with a nonlinear atomic medium.[18,19]

The quantum emission properties of the proposed system are quantitatively studied by means of the master equation for the coupled exciton and cavity photon fields including losses. In particular, we have studied the behavior of the second-order coherence function $g^{(2)}$ as a function of the relevant physical parameters and we have identified the regimes where the antibunching is most effective. These results are then used to characterize the emission in the presence of a pulsed source, which is shown to provide a train of single-photon pulses.

We start our theoretical treatment by recalling the quantum Hamiltonian model[12–14] describing a quantum well exciton strongly coupled to a planar microcavity photon mode, namely

$$\begin{aligned} H = & \int d\mathbf{x} \sum_{i,j\in\{X,C\}} \hat{\Psi}_i^\dagger(\mathbf{x}) h_{i,j}^0(-i\nabla)\hat{\Psi}_j(\mathbf{x}) \\ & + \frac{\hbar\kappa}{2}\int d\mathbf{x}\hat{\Psi}_X^\dagger(\mathbf{x})\hat{\Psi}_X^\dagger(\mathbf{x})\hat{\Psi}_X(\mathbf{x})\hat{\Psi}_X(\mathbf{x}) \\ & - \frac{\hbar\Omega_R}{n_{sat}}\int d\mathbf{x}\hat{\Psi}_C^\dagger(\mathbf{x})\hat{\Psi}_X^\dagger(\mathbf{x})\hat{\Psi}_X(\mathbf{x})\hat{\Psi}_X(\mathbf{x}) + h.c \\ & + \int d\mathbf{x}\hbar F_p(\mathbf{x},t)e^{-i\omega_p t}\hat{\Psi}_C^\dagger(\mathbf{x}) + h.c, \end{aligned} \tag{1}$$

where the field operators $\hat{\Psi}_{X,C}$ describe excitons (X) and cavity photons (C). These operators depend on the in-plane position wavevector $\mathbf{x}$, which is perpendicular to the growth direction z. They satisfy Bose commutation rules $[\hat{\Psi}_i(\mathbf{x}),\hat{\Psi}_j^\dagger(\mathbf{x}')]=\delta^2(\mathbf{x}-\mathbf{x}')\delta_{i,j}$. The linear term, including the exciton and planar microcavity photon kinetic energy (the motion along z is quantized), reads

$$h^0(-i\nabla) = \hbar\begin{pmatrix} \omega_X(-i\nabla) & \Omega_R \\ \Omega_R & \omega_C(-i\nabla)+V_C(\mathbf{x}) \end{pmatrix}, \tag{2}$$

where the exciton-photon coupling, responsible for the appearance of the polariton eigenmodes, is quantified by the vacuum Rabi frequency Ω_R. $V_C(\mathbf{x})$ describes the photonic dot confining potential due to the lithographic patterning. Two contributions are responsible for the polariton nonlinearities, namely the exciton-exciton interaction (modeled through a repulsive contact interaction potential with strength $\hbar\kappa$) and the anharmonic exciton-photon coupling (depending on the exciton oscillator strength saturation density n_{sat}). Finally, $F_p(\mathbf{x},t)$ describes the applied excitation field with frequency ω_p. The photon field operator can be expanded in terms of the confined modes in the photonic dot, namely $\hat{\Psi}_C(\mathbf{x}) = \Sigma_j \phi_{C,j}(\mathbf{x})\hat{a}_j$, where $\phi_{C,j}$ is the normalized wave function of the jth mode of energy $\hbar\omega_{C,j}^{dot}$, and $\hat{a}_j$ is the corresponding annihilation operator. Since the exciton kinetic energy is negligible compared to the photonic one (i.e., the wavevector dependence of ω_X is negligible compared to the one of ω_C),

it is convenient to use the same basis to expand the exciton operator as $\hat{\Psi}_X(\mathbf{x})=\Sigma_j \phi_{C,j}(\mathbf{x})\hat{b}_j$, where $\hat{b}_j$ is the corresponding bosonic exciton annihilation operator. In fact, it can be easily seen from Eq. (2) that each photon mode is coupled only to the exciton mode with the same spatial wave function, implying that the polariton eigenmodes have the same spatial wave function as the photonic dot modes.

In the following, we will be interested in studying the dynamics of the fundamental photonic mode confined in the photonic dot strongly coupled to the exciton level. In the case of a strong photonic confinement, the energy spacing between confined photon modes can become much larger than the mode spectral linewidth and the energy detuning between the quantum well exciton resonance and the considered photon mode. In this limit and for quasi-resonant excitation, we can safely simplify our quantum description by retaining in the Hamiltonian only the fundamental photonic dot mode of energy $\hbar\omega_C^{dot}$ and the exciton mode having the same spatial wave function $\phi_C(\mathbf{x})$. Thus, in the following, we will consider the following effective Hamiltonian:

$$H_{eff}=\hbar\omega_X b^\dagger b+\hbar\omega_C^{dot}a^\dagger a+\hbar\Omega_R b^\dagger a+\hbar\Omega_R b a^\dagger + \frac{\hbar\omega_{nl}}{2}b^\dagger b^\dagger bb-\alpha_{sat}\hbar\Omega_R b^\dagger b^\dagger ab-\alpha_{sat}\hbar\Omega_R a^\dagger b^\dagger bb + \hbar\mathcal{F}_0(t)e^{-i\omega_p t}a^\dagger+\hbar\mathcal{F}_0^*(t)e^{i\omega_p t}a, \quad (3)$$

where a and b are the bosonic annihilation operators of the considered photonic dot and exciton mode, respectively. The parameters involved in the effective Hamiltonian are the applied laser amplitude $\mathcal{F}_0(t)=\int d\mathbf{x}F_p(\mathbf{x},t)\phi_C{}^*(\mathbf{x})$, while $\alpha_{sat}=\frac{1}{n_{sat}}\int d\mathbf{x}|\phi_C(\mathbf{x})|^4$ and $\omega_{nl}=\kappa\int d\mathbf{x}|\phi_C(\mathbf{x})|^4$ are the effective nonlinear coefficients. The saturation coefficient α_{sat} will be neglected in the numerical solution because $\frac{\alpha_{sat}\hbar\Omega_R}{\hbar\omega_{nl}/2}=\frac{2\Omega_R}{n_{sat}\kappa}\ll 1$ for typical III-V microcavity parameters.[12]

To give the dependance of the nonlinear coefficient ω_{nl} on the photonic dot confinement, we have considered two simple geometries with infinite confinement barriers. In the case of a square dot, the normalized wave function is $\phi(x,y)=\frac{2}{L}\sin\left(\frac{\pi}{L}x\right)\sin\left(\frac{\pi}{L}y\right)$ where L is the lateral size. In the cylindrical case, $\phi(r)=\frac{1.087}{R}J_0(2.405r/R)$ where R is the radius of the cylinder and J_0 the zeroth-order Bessel function. The values of the geometric coefficients are $\int_{square}d\mathbf{x}|\phi_C(\mathbf{x})|^4=2.25/L^2$, and $\int_{cylinder}d\mathbf{x}|\phi_C(\mathbf{x})|^4=2.67/(2R)^2$, showing the inverse proportionality between ω_{nl} and the lateral area of the photonic mode. In order to study the quantum dynamics, it is convenient to work in the rotating frame described by the unitary operator $R(t)=e^{i(\omega_p t(a^\dagger a+b^\dagger b))}$. The rotating frame Hamiltonian is:

$$\tilde{H}_{eff}=\hbar\Delta\omega_X b^\dagger b+\hbar\Delta\omega_C a^\dagger a+\hbar\Omega_R b^\dagger a+\hbar\Omega_R b a^\dagger + \frac{\hbar\omega_{nl}}{2}b^\dagger b^\dagger bb+\hbar\mathcal{F}_0(t)a^\dagger+\hbar\mathcal{F}_0^*(t)a, \quad (4)$$

where $\Delta\omega_C=\omega_C^{dot}-\omega_p$ and $\Delta\omega_X=\omega_X-\omega_p$, respectively. To describe the quantum dynamics in presence of damping, we have considered the master equation for the rotating frame density matrix $\tilde{\rho}(t)=R(t)\rho(t)R^\dagger(t)$:

$$\frac{\partial\tilde{\rho}}{\partial t}=\frac{i}{\hbar}[\tilde{\rho},\tilde{H}_{eff}]+\gamma_C(a\tilde{\rho}a^\dagger-1/2(a^\dagger a\tilde{\rho}+\tilde{\rho}a^\dagger a)) + \gamma_X(b\tilde{\rho}b^\dagger-1/2(b^\dagger b\tilde{\rho}+\tilde{\rho}b^\dagger b)), \quad (5)$$

where γ_X and γ_C are the homogeneous broadening of the exciton and photon modes. The master equation can be solved by expanding the density matrix over a Fock basis, namely

$$\tilde{\rho}(t)=\sum_{n'_X,n'_C,n_X,n_C}\tilde{\rho}_{n'_X,n'_C,n_X,n_C}(t)|n'_X,n'_C\rangle\langle n_X,n_C|, \quad (6)$$

where n_X and n_C are the number of excitons and photons, respectively. In the following, we will be interested in the two-time second-order coherence function,[20] defined as:

$$g^{(2)}_{phot}(t,t')=\frac{G^{(2)}_{phot}(t,t')}{N_{ph}(t)N_{ph}(t')}=\frac{Tr(a\mathcal{U}_{t,t'}[a\tilde{\rho}(t')a^\dagger]a^\dagger)}{Tr(a\tilde{\rho}(t)a^\dagger)Tr(a\tilde{\rho}(t')a^\dagger)} =\frac{\sum_{m,n}m\theta_{n,m,n,m}(t,t')}{\sum_{m,n}m\tilde{\rho}_{n,m,n,m}(t)\sum_{m,n}m\tilde{\rho}_{n,m,n,m}(t')}, \quad \forall\, t>t'$$

$$\theta(t,t')=\mathcal{U}_{t,t'}\left[\sum_{n,m,n',m'}\tilde{\rho}_{n',m',n,m}(t')\sqrt{mm'}|n',m'-1\rangle \times\langle n,m-1|\right], \quad (7)$$

where $\mathcal{U}_{t,t'}$ is the evolution superoperator associated to the master equation (5).

As we have already discussed, we will consider the case of an applied optical field with frequency ω_p close to the frequency $\omega_{LP}^{dot}=\frac{\omega_C^{dot}+\omega_X}{2}-\sqrt{\Omega_R^2+\frac{(\omega_C^{dot}-\omega_X)^2}{4}}$ of the fundamental confined polariton mode in the dot. In the case of a continuous wave excitation, we give in Fig. 1 an example of the dependence of the equal-time second-order coherence

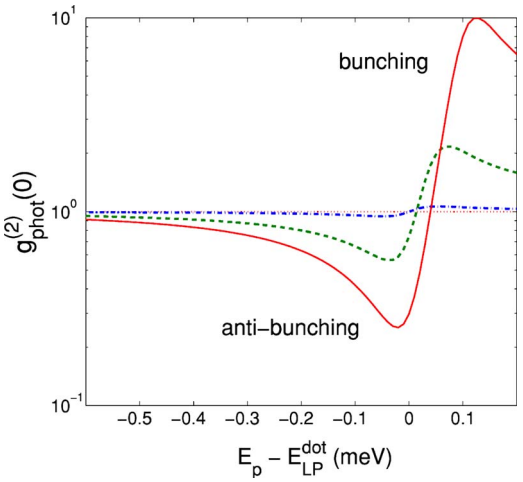

FIG. 1. (Color online) Intra-cavity second-order coherence function $g^{(2)}(0)$ vs pump detuning $\hbar\omega_p-\hbar\omega_{LP}^{dot}$ (meV) for three different cavity-exciton detunings. Solid, dashed, dotted-dashed line: $\hbar(\omega_C^{dot}-\omega_X)=5,\ 0,\ -5$ meV. Parameters: $\hbar\omega_{nl}=0.4$ meV, $\hbar\gamma_X=\hbar\gamma_C=0.1$ meV, $\hbar\Omega_R=2.5$ meV and continuous wave excitation field $\hbar\mathcal{F}_0=10^{-2}$ meV.

$g^{(2)}_{phot}(0) \equiv g^{(2)}_{phot}(t,t)$ on the laser excitation detuning $\omega_p - \omega^{dot}_{LP}$ for a given set of parameters. For a laser frequency red-detuned or close to resonance with the fundamental polariton resonance, $g^{(2)}_{phot}(0) < 1$, implying sub-Poissonian statistics and antibunching. This is the regime where the polariton quantum blockade is working. Indeed, the photon injection is inhibited when only a small number of polaritons are already inside the dot due to the interaction-induced blueshift of the polariton resonance. For large values of ω_{nl}/γ, only one polariton can be present in the photonic dot with a vanishing probability of having two at the same time, implying $g^{(2)}_{phot}(0) \approx 0$. On the other-hand, for a blue-detuned laser, the absorption resonance gets closer to the pump frequency. Thus the photon injection is enhanced by the nonlinear effect and $g^{(2)}_{phot}(0) > 1$, implying bunching. In Fig. 1, there are three curves corresponding to different detunings $\delta = \hbar(\omega^{dot}_C - \omega_X)$. Since the nonlinearity is due to the excitonic fraction of the polaritonic mode, the photonic antibunching is more pronounced for $\delta > 0$ because the nonlinearity is due to the excitonic component of the lower polariton mode that is quasiresonantly excited. Note that in the calculations reported here we have limited ourselves to moderately positive detunings δ, when the photonic content remains still significant (larger than 15%). The model here presented would not be in fact applicable for very large positive detunings when the energy separation between the lower polariton mode and the bare exciton level is comparable to the linewidth. In this regime, our single-mode approximation is no longer valid and one should consider also the localized exciton states induced by the experimentally unavoidable disordered excitonic potential. By contrast, for negative or moderately positive detunings δ, there is a considerable spectral separation between the lower polariton mode and the localized exciton states, which are very weakly coupled to the photon states.[21] Hence, for resonant excitation of the lower polariton mode, the role of disorder can be disregarded in first approximation. Even for detuning as large as $\delta = 5$ meV, the localized exciton states are still spectrally separated from the lower polariton by $E_{LP} - E_X = 1$ meV, i.e., ten times the linewidth γ.

As shown in Fig. 2, the minimum value of $g^{(2)}_{phot}(0)$ depends critically on the ratio ω_{nl}/γ, where the polariton mode linewidth $\gamma = |X_{LP}|^2\gamma_X + |C_{LP}|^2\gamma_C$, $|X_{LP}|^2$ and $|C_{LP}|^2$ being, respectively, the excitonic and photonic fractions of the lower

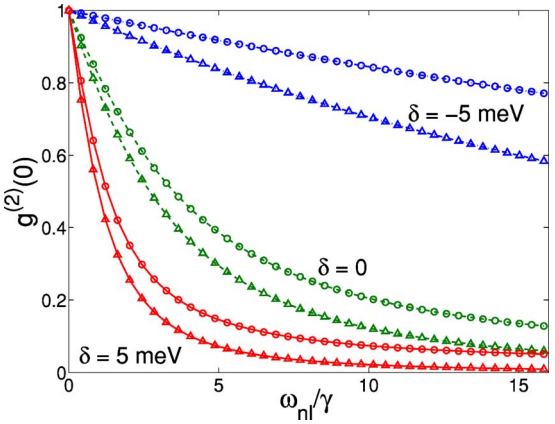

FIG. 2. (Color online) Second-order coherence function $g^{(2)}(0)$ for the photon (circles) and exciton (triangles) as a function of the normalized nonlinear coefficient ω_{nl}/γ for three different values of $\delta = \hbar(\omega^{dot}_C - \omega_X)$. Parameters: $\hbar\gamma_X = \hbar\gamma_C = 0.1$ meV and $\omega^{dot}_{LP} = \omega_p$.

polariton mode. Here, for the sake of clarity, calculations have been performed for $\gamma_X = \gamma_C = \gamma$. The antibunching behavior ($g^{(2)}_{phot}(0) < 1$) starts to be significant when $\omega_{nl}/\gamma \sim 1$. In order to have $\omega_{nl}/\gamma = 1$, with a polariton linewidth $\hbar\gamma = 0.1$ meV and a realistic nonlinear coefficient[12,13] $\hbar\kappa = 1.5 \times 10^{-2}$ $(\mu\text{m})^2$ meV (corresponding to an exciton blueshift of 0.15 meV in presence of 10^9 cm^{-2} excitons), a cylindrical dot with diameter $2R = 0.67$ μm would be required. Reducing further the size allows one to enter the strong quantum blockade regime $\omega_{nl}/\gamma \gg 1$. For example, using the same nonlinear coefficient, a square dot with lateral size $L = 0.2$ μm gives $\omega_{nl}/\gamma = 8.4$. In general, there is slight asymmetry between the photonic and excitonic antibunching ($g^{(2)}_{phot}(0) > g^{(2)}_{exc}(0)$) even at zero detuning. This asymmetry occurs because the nonlinearity is due to the exciton.

Given the current interest for single photon sources, it is interesting to characterize the figures of merit of the present system as a nonclassical source. In a transmission geometry, the coherence properties of the in-cavity polariton field [e.g., the second-order one (7)] transfer to the emitted field.[22] For any application it is important to maximize the photon population N_{ph}, keeping the sub-Poissonian character strong: In Fig. 3(a) we have plotted $g^{(2)}_{phot}(0)$ and the intra-cavity photon population N_{ph} as a function of the normalized incident intensity $|\mathcal{F}_0|^2/\gamma^2$ of the cw laser. For $|\mathcal{F}_0|^2/\gamma^2 \to 0$, $g^{(2)}_{phot}(0)$

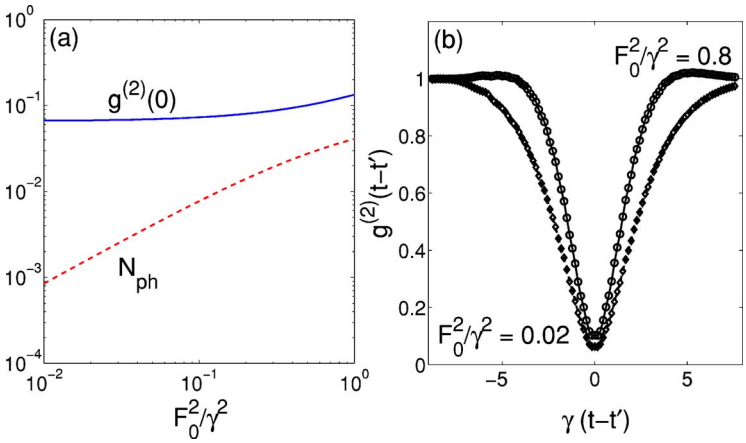

FIG. 3. (Color online) (a) Second-order coherence function $g^{(2)}_{phot}(0)$ (solid line) and intracavity photon population (dotted line) inside the dot as a function of pump power in the continuous wave regime. (b) Second-order coherence function $g^{(2)}_{phot}(t,t')$ at a fixed t' as a function of time for two different pump powers. Parameters: $\delta = \hbar(\omega^{dot}_C - \omega_X) = 5$ meV, $\hbar\omega_{nl} = 1$ meV, $\hbar\gamma_X = \hbar\gamma_C = 0.1$ meV.

asymptotically converges to a minimum value, but also the population N_{ph} goes to 0. For increasing $|\mathcal{F}_0|^2/\gamma^2$, N_{ph} increases, but $g^{(2)}_{phot}(0)$ eventually grows up. For the parameters here used, the crossover occurs for $N_{ph}\approx 0.01$. In Fig. 3(b), the dependence of $g^{(2)}_{phot}(t,t')$ on the relative time $t-t'$ is shown for two excitation intensities. It is apparent that the temporal width of the antibunching dip is directly related to the inverse polariton linewidth $1/\gamma$, at least in the limit $|\mathcal{F}_0|^2/\gamma^2 \to 0$.

Since the polariton quantum blockade effect relies on the resonant character of the excitation, one can wonder whether the effect is robust even in the pulsed excitation regime. In addition to the strong sub-Poissonian photon statistics, the efficiency and the repetition rate are the relevant quantities in the pulsed excitation case. We have solved the dynamics using a train of excitation pulses and we have found that by using Fourier-limited pulses with spectral linewidth comparable to the polariton one and a repetition rate $\Gamma \ll \gamma$, the suppression of the two-photon probability approaches the cw case. As an illustrative example, in Fig. 4(a) we show the time-dependent second-order correlation function $G^{(2)}_{phot}(t,t')$. The depletion of the central peak (which would not occur for a source with poissonian statistics, such as an attenuated laser beam) demonstrates the single-photon character of the present source even in the pulsed regime. The quantity $\eta=\gamma_C\int_{\Delta T} N_{ph}(t)dt$ (where ΔT is the time interval between two consecutive pulses) represents the averaged number of photons emitted per pulse. As shown in Fig. 4(b), a repetition rate $\Gamma=\gamma/10$ is enough to avoid pulse overlap. The effective quantum bit exchange rate of the present quantum source would be $r=\eta\Gamma$. With respect to the example in Fig. 4(b), we have $\eta\simeq 0.01$, implying a rate r as large as $r\simeq 0.1$ GHz.

In conclusion, the present work has predicted the rich quantum nonlinear dynamics of a quantum well exciton transition strongly coupled to a photonic quantum dot mode, showing the potential for the realization of a nonclassical light source with controllable properties based on the polariton quantum blockade effect.

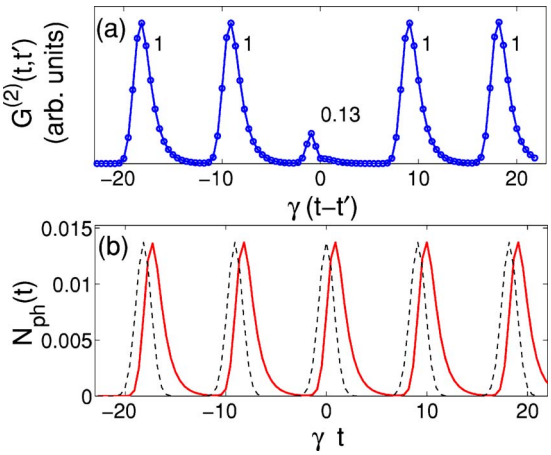

FIG. 4. (Color online) (a) Second-order correlation function $G^{(2)}_{phot}(t,t')$ for $t'=6$ ps under the excitation of a train of Gaussian pulses (pulse duration of 5 ps) separated from each other by 60 ps. The normalized area is indicated for each peak. (b) Corresponding intra-cavity photon population $N_{ph}(t)$. Dotted line: Shape of the pump amplitude $\mathcal{F}_0(t)$. Parameters: $\hbar(\omega_C^{dot}-\omega_X)=5$ meV, $\hbar(\omega_p-\omega_{LP}^{dot})=-0.05$ meV, $\hbar\omega_{nl}=1.1$ meV, $|\mathcal{F}_0|^2/\gamma^2=0.09$, $\hbar\gamma_X=\hbar\gamma_C=0.1$ meV, so $1/\gamma=6.6$ ps.

We thank G. Bastard, B. Deveaud, C. Diederichs, G. Dasbach, O. El Daïf, I. Favero, J.M. Gérard, F. Morier-Genoud, A. Imamoğlu, N. Regnault, and J. Tignon for discussions. LPA-ENS is a "Unité Mixte de Recherche Associé au CNRS (UMR 8551) et aux Universités Paris 6 et 7."

*Electronic address: ciuti@lpa.ens.fr

[1] *The Physics of Quantum Information*, edited by D. Bouwmeester, A. Ekert, and A. Zeilinger (Springer-Verlag, Berlin, 2000).
[2] N. Gisin *et al.*, Rev. Mod. Phys. **74**, 145 (2002).
[3] A. Beveratos, R. Brouri, T. Gacoin, A. Villing, J. P. Poizat, and P. Grangier, Phys. Rev. Lett. **89**, 187901 (2002).
[4] J. M. Gérard, B. Sermage, B. Gayral, B. Legrand, E. Costard, and V. Thierry-Mieg, Phys. Rev. Lett. **81**, 1110 (1998).
[5] P. Michler *et al.*, Science **290**, 2282 (2000).
[6] J. Kim *et al.*, Nature (London) **397**, 500 (1999); C. Santori *et al.*, *ibid.* **419**, 594 (2002).
[7] A. Badolato *et al.*, Science **308**, 1158 (2005).
[8] J. I. Perea, D. Porras, and C. Tejedor, Phys. Rev. B **70**, 115304 (2004).
[9] P. G. Savvidis, J. J. Baumberg, R. M. Stevenson, M. S. Skolnick, D. M. Whittaker, and J. S. Robe, Phys. Rev. Lett. **84**, 1547 (2000).
[10] C. Ciuti, P. Schwendimann, B. Deveaud, and A. Quattropani, Phys. Rev. B **62**, R4825 (2000).
[11] M. Saba *et al.*, Nature (London) **414**, 731 (2001).
[12] J. Baumberg and L. Viña, Semicond. Sci. Technol. **18**, S279 (2003).
[13] B. Deveaud, Phys. Status Solidi B **242**, 2145 (2005), and references therein.
[14] I. Carusotto and C. Ciuti, Phys. Rev. Lett. **93**, 166401 (2004).
[15] G. Dasbach, M. Schwab, M. Bayer, and A. Forchel, Phys. Rev. B **64**, 201309(R) (2001).
[16] O. El Daïf *et al.*, Appl. Phys. Lett. **88**, 061105 (2006).
[17] I. Carusotto, Phys. Rev. A **63**, 023610 (2001).
[18] A. Imamoğlu, H. Schmidt, G. Woods, and M. Deutsch, Phys. Rev. Lett. **79**, 1467 (1997).
[19] K. M. Bimbaum *et al.*, Nature (London) **436**, 87 (2005).
[20] D. F. Walls and G. J. Milburn, *Quantum Optics* (Springer-Verlag, Berlin, 1994).
[21] D. M. Whittaker, Phys. Rev. Lett. **80**, 4791 (1998); D. M. Whittaker, Phys. Rev. B **61**, R2433 (2000).
[22] In a monolithyc photonic structure as in Ref. 16, the spectral separation between the photonic dot modes and the planar cavity ones helps suppressing the contamination of the transmitted nonclassical output by excitation photons which have not been injected into the photonic dot. In fact, a resonant excitation beam with frequency close to the photonic dot lower polariton level cannot excite the higher energy planar cavity modes.